THE ASTROPHYSICAL JOURNAL, 531:321–328, 2000 March 1

LINE OSCILLATOR STRENGTH MEASUREMENTS IN THE 0–0 BAND OF THE $c'_4\,{}^1\Sigma_u^+ \leftarrow X^1\Sigma_g^+$ TRANSITION OF N_2

G. STARK,[1] K. P. HUBER,[2,3] K. YOSHINO,[4] M.-C. CHAN,[2,5] T. MATSUI,[6] PETER L. SMITH,[7] AND K. ITO[8]

Received 1999 August 13; accepted 1999 October 7

ABSTRACT

Oscillator strengths for 48 rotational lines in the 0–0 band of the $c'_4\,{}^1\Sigma_u^+ \leftarrow X^1\Sigma_g^+$ transition of $^{14}N_2$, a prominent feature in planetary airglow emissions, have been determined from vacuum ultraviolet photoabsorption spectra recorded with an instrumental resolution of $\sim 6.5 \times 10^{-4}$ nm (resolving power $\approx 150{,}000$). The sum of the integrated cross sections over all measured lines, including six lines appearing on account of a local perturbation by $v = 1$ of the b' state, yields a room temperature band f-value of 0.136 ± 0.020. This result is compared with earlier measurements of band-integrated absorption cross sections and with a study of electron-impact-induced emission from $c'_4(0)$, as well as with electron scattering measurements and a nonadiabatic calculation of vibronic band strengths. The relative P- and R-branch absorption intensities deviate systematically from those of an unperturbed $^1\Sigma \leftarrow {}^1\Sigma$ band, as expected from the interactions of the c'_4 ($v = 0$) level with nearby Rydberg and valence states. In addition, the variation of the band f-values derived from pairs of R- and P-branch transitions with a common lower-state rotational level, $f(J'')$, are found to be J-dependent, indicating that the f-value obtained from the band-integrated absorption cross section is slightly temperature dependent. The J-dependence of $f(J'')$ is briefly discussed in the context of the interference patterns which characterize the absorption strengths in the region of the widespread interactions between Rydberg and valence state levels.

Subject headings: ISM: molecules — molecular data — planets and satellites: general — ultraviolet: general

1. INTRODUCTION

Molecular nitrogen airglow emissions in the vacuum ultraviolet (VUV) and extreme ultraviolet (EUV) regions, both from the Earth's atmosphere (Meier 1991) and from the atmospheres of the planetary satellites Titan and Triton (e.g., Strobel & Shemansky 1982; Broadfoot et al. 1989), have been extensively observed. The most prominent EUV emission features in the airglows of Titan and Triton, where N_2 is the major atmospheric constituent, originate from the $v = 0$ level of the $c'_4\,{}^1\Sigma_u^+$ Rydberg state of N_2. The primary excitation mechanism in these atmospheres is electron collisions, and the relative strengths of the $c'_4(0)$ atmospheric emissions are consistent with the fact that the c'_4–X 0–0 band at 95.86 nm has the largest measured electron excitation cross section for N_2 emission (Ajello et al. 1989).

The $c'_4(0)$ emissions are found to be much weaker in the Earth's airglow (e.g., Christensen 1976). Stevens et al. (1994) developed a comprehensive radiative transfer model of the $c'_4(0)$ emissions which successfully accounted for the main features of this airglow. Such comprehensive interpretations of airglow observations require an accurate and complete spectroscopic database; for the $c'_4(0)$ bands this includes line positions, line oscillator strengths, predissociation probabilities, and radiative branching ratios. Despite considerable experimental and theoretical efforts, significant uncertainties and gaps remain in the spectroscopic database. For example, band f-values for the 0–0 band of $c'_4 \leftarrow X$ have been measured but individual line f-values have not, and, because of perturbations in the $c'_4(0)$ level, line f-values cannot be reliably calculated from the band f-value. This paper reports new photoabsorption measurements of 48 rotational line oscillator strengths in the 0–0 band and of six lines associated with the interacting $b'(1)$ valence state level. The (0–0) band is the strongest N_2 absorption feature in the EUV region. The measured f-values for the lowest-J lines in the band will also prove useful in the search for interstellar N_2 absorption features from the NASA *Far Ultraviolet Spectroscopic Explorer* (*FUSE*) satellite.

The dipole-allowed absorption spectrum of N_2 at wavelengths shortward of 100 nm arises from transitions to the perturbed vibrational progressions of three Rydberg and two valence states (Dressler 1969; Carroll & Collins 1969; Lefebvre-Brion 1969). The $c'_4\,{}^1\Sigma_u^+$ state is the lowest member of the $np\sigma$ series converging to the $X^2\Sigma_g^+$ ground state of N_2^+ (Carroll & Yoshino 1967; Carroll, Collins, & Yoshino 1970; Carroll & Yoshino 1972; Yoshino, Freeman, & Tanaka 1979); together with the nearby $c_3(0)^1\Pi_u$ level, it forms the lowest p Rydberg complex. Yoshino & Tanaka (1977) analyzed the rotational structure of the $c'_4 \leftarrow X$ 0–0 band and showed its peculiar "doubled-headed" structure to be caused by a homogeneous interaction of $c'_4(0)$ with $v = 1$ of the $b'^1\Sigma_u^+$ valence state. Levelt & Ubachs (1992),

[1] Department of Physics, Wellesley College, 106 Central Street, Wellesley, MA 02481; gstark@wellesley.edu.

[2] Institute for Astrophysics and Planetary Sciences, Faculty of Science, Ibaraki University, 2-1-1 Bunkyo, Mito 310-8512, Japan.

[3] Permanent address: Steacie Institute for Molecular Sciences, National Research Council, Ottawa, Ontario, K1A 0R6, Canada; klaus.huber@nrc.ca.

[4] Harvard-Smithsonian Center for Astrophysics, 60 Garden Street, Cambridge, MA 02138; kyoshino@cfa.harvard.edu.

[5] Permanent address: Department of Chemistry, The Chinese University of Hong Kong, Shatin, N.T., Hong Kong; mcc@gundam.chem.cuhk.edu.hk.

[6] Hiroshima Synchrotron Radiation Center, Hiroshima University, 2-313 Kagamiyama, Higashi-Hiroshima, 739-8526, Japan; matsuit@hisor.material.sci.hiroshima-u.ac.jp.

[7] CURSOAR Technologies, 93 Pleasant Street, Watertown, MA 02171-2317 and Harvard-Smithsonian Center for Astrophysics, 60 Garden Street, Cambridge, MA 02138; p1smith@cfa.harvard.edu.

[8] Photon Factory, Institute for Materials Structure Science, High Energy Accelerator Research Organization, 1-1 Oho, Tsukuka, Ibaraki, 305-0801, Japan; kenji.ito@kek.jp.

using a high-resolution EUV laser apparatus, improved the accuracy of the line position measurements; also, their data reduction allows for ℓ-uncoupling interactions within the p complex, although not in a completely rigorous fashion.

Stahel, Leoni, & Dressler (1983), in their comprehensive treatment of homogeneous Rydberg-Rydberg and Rydberg-valence interactions in N_2, showed that the $c_3(0)$ level is strongly mixed with the vibrational levels of the $b^1\Pi_u$ valence state; hence a complete analysis of the $c'_4(0)$ rotational structure must include not only interactions with the $b'(1)$ and $c_3(0)$ levels, but also the $c_3(0) \sim b(v)$ interactions. Edwards et al. (1995) extended the analysis of Stahel et al. (1983) by including the effects of nuclear rotation; their calculation of the percentage electronic character for $c'_4(0)$ rotational levels with $J < 30$ (see Table 1 in Edwards et al. 1995) confirms that the high-J levels are significantly mixed with e parity levels of both $c_3\,{}^1\Pi_u$ and $b^1\Pi_u$. The strengths of individual rotational transitions in the $c'_4 \leftarrow X$ 0–0 band, never measured and reported before, are affected by the complex interactions of the excited singlet states, and simple spectroscopic models cannot account for the observed distribution of line strengths within the band.

Previous $c'_4(0)$–$X(0)$ oscillator strengths have been reported from electron scattering and photoabsorption measurements. Geiger & Schröder (1969) reported relative intensities in the N_2 energy-loss spectrum of 25 keV electrons at a resolution of 10 meV ($\approx$0.074 nm at 95.8 nm); after correction for the scattering geometry, these intensities can be converted to relative band oscillator strengths (Stahel et al. 1983). Chan et al. (1993) determined absolute N_2 band f-values from energy-loss spectra of 8 keV electrons at a resolution of 48 meV ($\approx$0.36 nm at 95.8 nm). In addition, Ajello et al. (1989) reported a 0–0 band f-value derived from their electron-impact studies of the emission-excitation cross section for the $c'_4(0)$ level.

Early EUV photoabsorption measurements of N_2 were carried out at relatively low-resolution. Lawrence, Mickey, & Dressler (1968) measured four bands with an instrumental resolution of $\sim$0.004 nm; Carter (1972) and Gürtler, Saile, & Koch (1977) surveyed the 73 to 99 nm and 66 to 99 nm regions, respectively, with instrumental resolutions of $\sim$0.004 and 0.003 nm. Optical absorption measurements provide, in principle, a direct determination of band f-values. However, as discussed by a number of authors (e.g., Hudson 1971; Stark et al. 1991; Chan, Cooper, & Brion 1991; Jolly et al. 1997), insufficient instrumental resolution complicates the analysis of saturated lines. The effects associated with insufficient instrumental resolution, if not minimized or properly accounted for, result in a systematic underestimation of integrated photoabsorption cross sections and oscillator strengths. Various experimental and analytic strategies can be used to minimize, or correct for, instrumental effects in an absorption measurement. However, there are unavoidable uncertainties associated with extracting f-values from low-resolution absorption measurements, and these uncertainties increase with decreasing instrumental resolving power.

Stark et al. (1992) reported oscillator strengths for seven N_2 bands between 95.8 and 99.4 nm from absorption spectra recorded with an instrumental resolution of $\sim 6.2 \times 10^{-4}$ nm, an approximately five-fold improvement over previous measurements. $c'_4(0) \leftarrow X(0)$ Doppler widths at room temperature are approximately 2.2×10^{-4} nm FWHM. In an effort to minimize instrumental resolution effects, the measurements of Stark et al. (1992) were limited to peak optical depths of $\leq$0.3, and corrections based on the analyses of synthetic absorption spectra convolved with the estimated instrumental line shape were applied to the measured band-integrated cross sections. While the instrumental resolution was sufficient to resolve all rotational features in the 0–0 band except those in the region of the R head (see Fig. 1g in Stark et al. 1992), the poor signal-to-noise ratio of measurements restricted to weak absorption features precluded the accurate determination of individual line f-values; only a band f-value was reported.

Since this work was completed, a number of laboratory investigations and spectroscopic analyses (Levelt & Ubachs 1992; Edwards et al. 1995; Shemansky, Kanik, & Ajello 1995; Ubachs 1997) and airglow models (Stevens et al. 1994; Stevens 1999, have focused on the determination of line positions, relative line strengths, line widths, and predissociation probabilities. Given the continued interest in the detailed spectroscopy of the $c'_4(0)$–$X(0)$ transition, and anticipating the search for N_2 absorption features in the interstellar medium, we have re-measured the absorption spectrum of this band. The same experimental apparatus was used as before (Stark et al. 1992, see § 2), with one significant improvement—the signal-to-noise ratio has been enhanced by a factor of three, allowing for accurate measurements of individual line strengths. We have also adopted an analysis technique (Lewis 1999, private communication) that accounts for instrumental resolution effects by a least-squares fitting of the measured absorption profiles to N_2 line profiles convolved with the instrumental function.

2. EXPERIMENTAL PROCEDURE

Photoabsorption measurements were made at the 2.5 GeV storage ring of the Photon Factory synchrotron radiation facility at the High Energy Accelerator Research Organization in Tsukuba, Japan. High spectral resolution was obtained with a 6.65 m spectrometer equipped with a photoelectric focal plane scanner (Ito et al. 1986, 1989). A zero-dispersion order sorter was used to reduce the bandpass of the continuum radiation entering the spectrometer to about 3 nm. A 1200 grooves mm^{-1} grating, blazed at 550 nm, was used in the sixth order to give a reciprocal dispersion of $\approx$0.02 nm mm^{-1}. Spectrometer entrance and exit slits of ~ 10 μm resulted in measured rotational line widths of $\sim 7 \times 10^{-4}$ nm. The instrumental resolution was approximately 6.5×10^{-4} nm, corresponding to a resolving power of 150,000. The determination of the instrumental profile is discussed in § 3.

The absorption measurements were made on molecular nitrogen in natural isotopic abundance ($^{14}N_2$ 99.3%, $^{14}N^{15}N$ 0.7%). The spectrometer tank, at a temperature of 295 K, served as an absorption cell with a path length of 12.49 m. In order to minimize saturation effects, the measured fractional absorption at the centers of the rotational lines was kept below $\sim$30%. This required relatively low spectrometer tank pressures. Absorption spectra were recorded with N_2 pressures ranging from 3.2×10^{-7} torr to 2.9×10^{-6} torr, corresponding to N_2 column densities ranging from 1.3×10^{13} cm^{-2} to 1.2×10^{14} cm^{-2}. At these pressures, outgassing from, and leaks through, the tank walls would have contaminated a static gas sample over the time of a full scan. Consequently, a flowing configuration was used. The spectrometer tank was continuously pumped

by a turbomolecular pump with a capacity of 1500 liters s^{-1}, while N_2 entered the tank through a needle valve. The tank pressure was monitored with an ionization gauge; the gauge calibration and the associated uncertainties in the N_2 column densities are discussed in § 3. At the pressures of interest, molecular flow conditions prevailed, ruling out the occurrence of pressure differentials that could have adversely affected the measurements. The limiting pressure in the spectrometer tank was $\sim 2.0 \times 10^{-7}$ torr; the composition of the residual gas was unknown, but the tank contents at this limiting pressure showed no signs of absorption at the wavelength of the $c'_4(0)$–$X(0)$ band.

All spectra were scanned at a speed of 0.0025 nm $minute^{-1}$. A signal integration time of about 1 s resulted in one data point for each 4.4×10^{-5} nm of the spectrum. Signal rates from the detector, a windowless solar-blind photomultiplier tube with a CsI-coated photocathode, were about 50,000 s^{-1} for the background continuum; the detector dark count rate was typically less than 2 s^{-1}. A signal-to-noise ratio of about 250 was achieved for the continuum level. Eleven scans of two overlapping portions of the 0–0 absorption spectrum between 95.805 and 96.002 nm were recorded, six scans covering the R-branch band head and the low-J lines in the R- and P-branches and five scans covering the high-J lines in the P-branch.

3. ANALYSES AND RESULTS

The eleven absorption spectra of the $c'_4(0)$–$X(0)$ band were converted to absorption cross sections through application of the Beer-Lambert law,

$$\sigma_M(\lambda) = \frac{1}{N} \ln \left[\frac{I_0(\lambda)}{I(\lambda)} \right], \tag{1}$$

where $\sigma_M(\lambda)$ is the measured absorption cross section, which includes the effects of the finite instrument resolution; N is the column density of N_2 molecules; $I_0(\lambda)$ is the background continuum level; and $I(\lambda)$ is the transmitted intensity. A correction for scattered light in the spectrometer, known to be less than 3% of $I_0(\lambda)$ (Ito et al. 1989), was not applied to the data. A representative measured absorption cross section of the band is shown in Figure 1.

A least-squares fitting routine, taking into account the effects of the finite instrumental resolution on each measured absorption feature, was used to determine values for the corrected integrated cross section of each line. At the low column densities used in the measurements, and with the exception of the R head region to be described below, there was negligible absorption between adjacent lines, allowing for the unambiguous determination of the background continuum level used in the fits. Typically, small variations in $I_0(\lambda)$ across individual lines amounted to less than 0.4% and were modeled in the fits by linear interpolation. Individual rotational lines were described by a Voigt profile. The Gaussian component is that of a Doppler broadened N_2 line at 295 K (2.2×10^{-4} nm FWHM). The Lorentzian component is taken from the recent measurements by Ubachs (1997) of 0–0 absorption lines terminating on the $J = 1$ and $J = 2$ levels of $c'_4(0)$. These widths were found to be slightly less than 1×10^{-5} nm (FWHM), and from the percentage electronic character calculated for rotational levels up to $J = 30$ (Edwards et al. 1995), there is no reason to expect that they will change substantially over the range of rotational quantum numbers observed in the present work, at least not for $J < 20$ where the only significant perturbation is due to $b'(1)$ whose levels according to Ubachs (1997) are approximately 16% narrower than in $c'_4(0)$. Above $J \approx 20$, the $c'_4(0)$ levels become increasingly mixed with the e parity levels of $b^1\Pi_u(v = 5)$ and, to a lesser extent, $c_3\,{}^1\Pi_u$ ($v = 0$). However, in the absence of definitive line width measurements at higher J, the Lorentzian component of the Voigt profiles for all rotational lines was set at 1×10^{-5} nm (FWHM). As shown below, uncertainties in this narrow Lorentzian width have a very small effect on the values of the integrated cross sections.

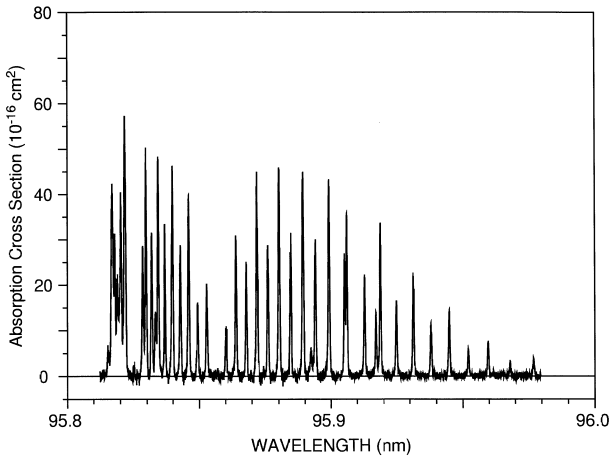

FIG. 1.—Representative uncorrected photoabsorption cross section of the $c'_4(0) \leftarrow X(0)$ band of $^{14}N_2$ at a temperature of 295 K. Because of instrumental distortion of the lines, the measured peak cross sections are lower limits to the correct values (see text).

The instrument function was also found to be best represented by a Voigt profile. For each line, its parameters were determined by fitting the measured absorption profile to the adopted line profile, the latter convolved with the instrument function. In any one scan, the resulting Gaussian and Lorentzian components of the instrument profile showed small variations from line to line. Weighted average widths of 5.2×10^{-4} and 2.3×10^{-4} nm, respectively, were used to construct the adopted instrument profile; with a FWHM of 6.5×10^{-4} nm, it was held fixed in subsequent iterations of the fitting routine. The estimated uncertainties associated with the instrument function will be discussed below. The final least-squares fits, based on the adopted line and instrument profiles, extracted optimized values for the true integrated cross section of each absorption line. An expanded view of the measured absorption cross sections for $R(0)$ and $R(1)$ is shown in Figure 2, together with the fitted cross sections and an indication of the FWHM for the averaged instrument profile.

The integrated cross sections of individual rotational lines, determined from the fitting procedure, were converted into line oscillator strengths according to (Morton & Noreau 1994)

$$f_{J',J''} = \left(\frac{4\varepsilon_0 m_e c^2}{e^2} \right) \frac{\int \sigma(\lambda) d\lambda}{\lambda^2 \alpha_{J''}}$$

$$= (1.1296 \times 10^3) \frac{\int \sigma(\lambda) d\lambda}{\lambda^2 \alpha_{J''}}, \tag{2}$$

where $\sigma(\lambda)$ and λ are measured in units of 10^{-16} cm^2 and nm, respectively, and $\alpha_{J''}$ is the fractional population of N_2

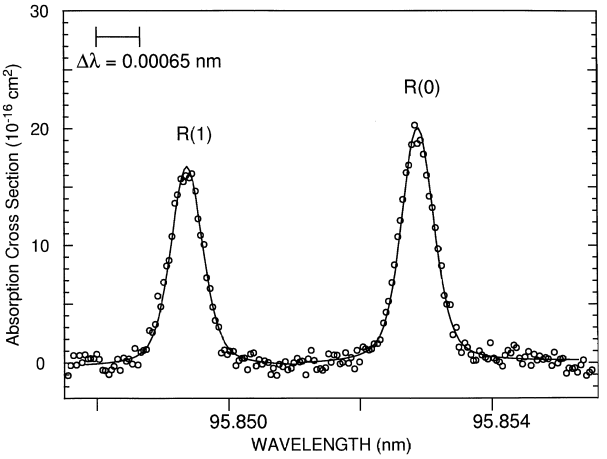

FIG. 2.—*Open circles*: Uncorrected measured photoabsorption cross sections of the $R(0)$ and $R(1)$ lines in the $c'_4(0) \leftarrow X(0)$ band of $^{14}N_2$. *Solid line*: Modeled cross sections from a least-squares fit. The spectrum was sampled at wavelength intervals of 4.4×10^{-5} nm. The instrumental resolution, $\Delta\lambda$, determined by the fitting routine, is also indicated.

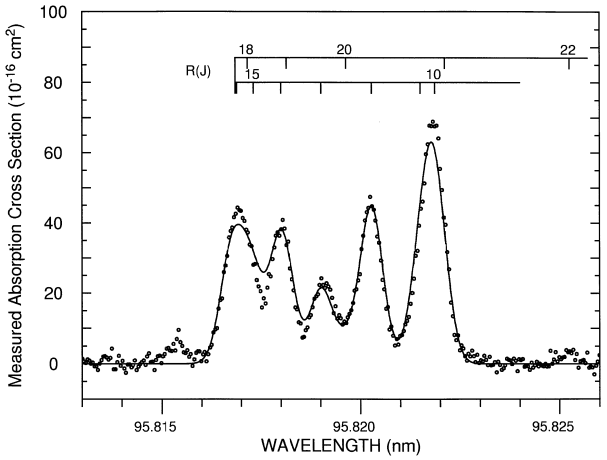

FIG. 3.—Uncorrected measured photoabsorption cross sections of $^{14}N_2$ (*open circles*) and modeled cross section (*solid line*) in the R head region of $c'_4(0) \leftarrow X(0)$. Estimated R line f-values initially used to generate the modeled spectrum were later rescaled for the model to match the resolution-corrected measured integrated cross section for the region (see text). The weak absorption feature at 95.8155 nm is the $R(9)$ line of the $b'(1) \leftarrow X(0)$ band.

molecules in the J'' rotational level as determined from a normalized Boltzmann factor based on N_2 ground-state term values (Edwards et al. 1993), and taking into account the 2:1 statistical weights of even and odd numbered lines due to nuclear spin. Most lines were measured at four different column densities, and the final line f-values represent appropriately weighted averages of these results. To minimize any errors associated with uncertainties in the adopted instrument profile, only absorption features with measured peak optical depths of less than 0.25 were included in the weighted averages.

The above analysis was applied to all well-resolved, unblended lines, i.e., to all P branch lines and to R branch lines with $J'' < 10$. However, because of its sensitivity to the exact positions of the lines, the least-squares fitting technique could not be applied to twelve blended lines in the R head region (see Fig. 3). Instead, integrated cross sections of the R head region were first determined from each of four absorption scans. In order to establish the effects of saturation on each integral, synthetic absorption spectra of the head region were generated from known line positions (Levelt & Ubachs 1992) and established term values (Edwards et al. 1993; Yoshino & Tanaka 1977), each $R(J'')$ line being given the adopted Voigt profile and an estimated oscillator strength derived from the measured f-value of the corresponding $P(J'')$ line and appropriate Hönl-London factors (Kovács 1969). An examination of the integrated *synthetic* cross sections before and after convolution with the instrument profile suggested that, depending on the column densities used to record the spectra, small corrections ranging from 2% to 8% had to be applied to the integrated *measured* cross sections. Finally, we re-scaled the estimated R-line f-values so as to match the integrated synthetic cross section with the weighted average of the integrated measured cross sections for the band head region. Figure 3 illustrated the satisfactory match of the observed with the calculated cross sections.

The f-values for all 48 measured lines in the 0–0 band, along with estimated uncertainties, are listed in Table 1. Table 2 contains similar data for six extra lines which

TABLE 1

$c'_4(0) \leftarrow X(0)$ LINE OSCILLATOR STRENGTHS[a]

J''	$P(J'')$	$R(J'')$
0	...	0.150(15)
1	0.051(10)	0.089(13)
2	0.056(6)	0.075(8)
3	0.060(6)	0.075(8)
4	0.064(13)	0.071(11)
5	0.063(6)	0.069(7)
6	0.064(13)	0.069(14)
7	0.064(6)	0.061(12)
8	0.069(14)	0.064(10)
9	0.066(10)	0.057(6)
10.....	0.071(11)	0.050(10)[b]
11.....	0.068(7)	0.056(11)[b]
12.....	0.061(12)	0.061(12)[b]
13.....	0.081(8)	0.065(13)[b]
14.....	0.080(12)	0.065(13)[b]
15.....	0.085(9)	0.068(14)[b]
16.....	0.082(8)	0.065(13)[b]
17.....	0.094(8)[c]	0.068(14)[b]
18.....	0.084(8)	0.067(13)[b]
19.....	0.088(9)	0.070(14)[b]
20.....	0.079(8)	0.062(12)[b]
21.....	0.084(17)	0.066(13)[b]
22.....	0.081(12)	0.065(13)
23.....	0.076(15)	
24.....	0.068(14)	
25.....	0.066(13)	

[a] Estimated uncertainties (in parentheses) in units of last quoted decimal place.

[b] f-values determined from corresponding P line f-values and appropriate Hönl-London factors, and scaled to match the integrated cross section of the R head region (see text, § 3).

[c] $P(17)$ is overlapped by the much weaker $P(13)$ line of $b'(1) \leftarrow X(0)$.

TABLE 2

$b'(1) \leftarrow X(0)$ LINE OSCILLATOR STRENGTHS[a]

J''	$P(J'')$	$R(J'')$
9.....	0.0013(3)	0.010(2)
10.....	0.0036(7)	0.015(3)
11.....	0.011(2)	
12.....	0.018(3)	

[a] Estimated uncertainties (in parentheses) in units of last quoted decimal place.

appear at intermediate J values on account of the local perturbation of $c'_4(0)$ by $b'(1)$.

Contributions to the estimated error limits associated with the line f-values in Tables 1 and 2 arise from uncertainties in the N_2 column densities, uncertainties associated with the adopted instrument profile of the spectrometer and the Lorentzian component of the Voigt profiles for individual lines, and from uncertainties in the parameters extracted by the least-squares fitting routine. For pressures greater than 2×10^{-6} torr, the ionization gauge monitoring the tank pressure was calibrated by volumetric expansion of N_2; a small volume, representing a measured fraction of the spectrometer tank volume and filled to pressures that could be measured with a capacitance manometer, was expanded into the main tank. We estimate that in this pressure range the N_2 column densities could be determined with an uncertainty of less than 10%.

At lower pressures, volumetric expansion becomes unreliable because of increasing uncertainties in the capacitance manometer readings, and because of the increasing importance of spectrometer tank outgassing which affects the total tank pressure during the time required for the N_2 gas expansion to equilibrate. At pressures below 2×10^{-6} torr, a calibration procedure relying on the comparison of integrated cross sections of individual lines was used to determine the column densities. First, the N_2 column for the highest-pressure scan (3.3×10^{-6} torr) was established via the volumetric expansion technique, and integrated cross sections for 12 high-J lines in the P-branch were determined from the fitting routine. These results were then used to derive from measurements of the same 12 P lines the column densities for four scans carries out at lower pressures, and a satisfactory linear gauge calibration for pressures from 0.78×10^{-6} to 3.3×10^{-6} torr was obtained from a least-squares fit to all five column densities. Next, the column density for a low-pressure scan (0.83×10^{-6} torr) of the low-J region was calculated using the gauge calibration, and integrated cross sections for the low-J lines were determined and then used to establish column densities for other low-J scans. A least-squares fit to the column densities of all eleven absorption scans produced the final linear gauge calibration.

Although deviations from the least-squares fit were small, we estimate the uncertainty in the N_2 column density to be as high as 30% for the lowest pressure, dropping to 5% for the highest pressure. An additional error is likely to arise from small drifts in the tank pressure over the course of an absorption scan, each scan requiring approximately 30 minutes of integration time. This effect was taken into account in the final estimates of the column density uncertainties.

The integrated cross sections of individual rotational lines, determined from the least-squares fitting procedure, depend on the assumed profiles of the instrument function and of the rotational lines. We estimate that the Gaussian (5.2×10^{-4} nm FWHM) and Lorentzian (2.3×10^{-4} nm FWHM) components of the adopted instrument Voigt profile have uncertainties of about $\pm 0.4 \times 10^{-4}$ and $\pm 0.8 \times 10^{-4}$ nm, respectively. The uncertainties are correlated such that the instrument Voigt function (6.5×10^{-4} nm FWHM) can be trusted to $\pm 0.5 \times 10^{-4}$ nm. This translates into integrated cross section uncertainties that range from $\sim 5\%$ for the weakest measured lines to $\sim 10\%$ for the strongest. Changes in the adopted Lorentzian component (1×10^{-5} nm FWHM) of the rotational lines produce very modest changes in the integrated cross sections; for example, a doubling of the Lorentzian component typically increases the integrated cross section of an individual line by $\sim 1\%$. The total uncertainties in individual line f-values from all sources, including statistical errors of the fitting parameters (typically $< 5\%$), are estimated to range from $\sim 10\%$ to $\sim 20\%$. For any one line, the f-values derived from separate absorption scans were generally found to scatter within much narrower limits. However, given the systematic nature of the column density and instrument profile uncertainties, it seems prudent to adopt the larger estimates.

4. DISCUSSION

For the purpose of comparing our results with previous measurements of band f-values for the $c'_4(0) \leftarrow X(0)$ transition, we have summed the integrated cross sections of all rotational lines observed and measured in this work, including the six $b'(1) \leftarrow X(0)$ lines in Table 2 which borrow their intensity from the much stronger $c'_4(0) \leftarrow X(0)$ band. The room temperature band-integrated cross section was converted into a band oscillator strength according to (Morton & Noreau 1994)

$$f = \frac{1.1296 \times 10^3 \int \sigma(\lambda) d\lambda}{\lambda^2}, \tag{3}$$

where λ was taken to be 95.856 nm, the position of the band origin. Our room temperature result, $f = 0.136 \pm 0.020$, is compared in Table 3 with other photoabsorption or emission measurements, electron energy loss experiments, and the nonadiabatic calculation of vibronic dipole strengths by Stahel et al. (1983). The absorption results of Carter (1972) and of Gürtler et al. (1977), where the systematic effects of inadequate spectral resolution were either ignored or only partially corrected for, are not included in the table.

Our band f-value is consistent with the early absorption measurements of Lawrence et al. (1968), who extrapolated their 0.004 nm resolution measurements to low column densities to minimize instrumental resolution effects. The current result is also in satisfactory agreement with our earlier result of 0.145 ± 0.030 (Stark et al. 1992).

In connection with a study of electron-impact excitation cross sections for emission from $c'_4(0)$, Ajello et al. (1989) reported a $c'_4(0) \leftarrow X(0)$ oscillator strength which is only marginally consistent with our new band f-value. There is even less agreement with f-values obtained from electron energy-loss measurements. In our previous work (Stark et al. 1992), the relative band f-values from the energy-loss spectra of Geiger & Schröder (1969) were placed on an

TABLE 3

COMPARISON OF $c'_4(0) \leftarrow X(0)$ BAND OSCILLATOR STRENGTHS[a]

Reference	Band f-value
Photoabsorption	
This work	0.136(20)[b]
Lawrence et al. 1968	0.14(4)
Stark et al. 1992	0.145(28)
Electron-impact-induced emission from $c'_4(0)$	
Ajello et al. 1989	0.156(30)
Electron Scattering	
Geiger & Schröder 1969.....	0.165[c]
Chan et al. 1993	0.195(20)
Calculation	
Stahel et al. 1983	0.153[d]

a Uncertainties (in parentheses, where available) in units of last quoted decimal place.

[b] As discussed in the text, this band f-value and all other measured values tabulated above are strictly appropriate only for room temperature.

[c] Electron energy loss measurements; normalized to $f = 0.044$ for $b(3) \leftarrow X(0)$ (see Stark et al. 1992).

[d] Nonadiabatic calculation of vibronic band strengths; normalized to $f = 0.046$ for $b(3) \leftarrow X(0)$ (see Stark et al. 1992).

absolute scale by normalizing to $f = 0.044$ for the $b(3) \leftarrow X(0)$ band, a choice which led to moderate agreement with our measurements of seven N_2 bands between 95.8 and 99.4 nm, but resulted in an oscillator strength of 0.165 for $c'_4(0) \leftarrow X(0)$ which now lies outside the error limits of our revised f-value.

The band f-value derived by Chan et al. (1993) from their electron scattering data is almost 50% larger than our result. The low resolution of their spectra, approximately 0.36 nm at 95.8 nm, results in overlapped signals from the 0–0 bands of $c'_4 \leftarrow X$ and $c_3 \leftarrow X$ and requires a deconvolution of the two transitions. Considering that the $c_3(0) \leftarrow X(0)$ f-value of Chan et al. (1993) is also larger than our result of 1992, it seems unlikely that uncertainties in the deconvolution of the two blended features are entirely responsible for the discrepancies between the f-values for $c'_4(0) \leftarrow X(0)$.

Stahel et al. (1983) calculated a set of relative vibronic band strengths for the dipole-allowed transitions of N_2 based on their nonadiabatic representation of the homogeneously mixed Rydberg and valence states. Relative electronic transition moments for the lowest parallel and perpendicular transitions from the $X\,^1\Sigma_g^+$ ground state were determined by fitting the squares of the perturbed vibronic transition moments to the relative dipole strengths derived from the electron energy-loss spectra of Geiger & Schröder (1969). Satisfactory agreement with our previous measurements in the 95.8 to 99.4 nm region (Stark et al. 1992) was obtained by normalizing the relative f-values derived from the calculations of Stahel et al. (1983) to $f = 0.046$ for the $b(3) \leftarrow X(0)$ band. For $c'_4(0) \leftarrow X(0)$, the calculated f-value of 0.153 is also within the error limits of our new experimental result. The work of Stahel et al. (1983) neglects the effects of heterogeneous interactions which introduce significant $^1\Pi_u$ character to the $c'_4(0)$ rotational levels of e parity (Edwards et al. 1995) and may affect the line strengths for $J > 20$.

The P/R ratios of the line f-values of $c'_4(0) \leftarrow X(0)$ are displayed in Figure 4. The effects of the $c'_4(0) \sim b'(1)$ interaction (Yoshino & Tanaka 1977; Levelt & Ubachs 1992) are very noticeable from the dispersion-like behavior of the f_P/f_R ratios near $J = 11$. Also shown in the figure are the smaller P/R ratios of the Hönl-London factors for an unperturbed $^1\Sigma$–$^1\Sigma$ band. The systematic deviations of the observed from the predicted ratios are reminiscent of similar observations in the emission spectrum (Shemansky et al. 1995) and are, in a qualitative sense, consistent with the description of $c'_4(0)$ as the upper component of a Rydberg p complex; line strength expressions have been discussed by Carroll (1973) and Johns (1974). However, the $^1\Pi_u$ lower component of the complex, $c_3(0)$, is itself strongly mixed with the $b\,^1\Pi_u$ valence state (Stahel et al. 1983; Edwards et al. 1995), thus adding to the difficulties faced in a quantitative analysis of the measured line strengths, particularly at the highest J values observed in this work.

In the absence of perturbations, the rotational line oscillator strengths, $f_{J',J''}$, and the band oscillator strength, f, for a $^1\Sigma$–$^1\Sigma$ transition are related (Morton & Noreau 1994) by

$$f = \frac{(2J'' + 1) f_{J',J''}}{S_{J',J''}}, \tag{4}$$

where the Hönl-London factors, $S_{J',J''}$, for P and R branch transition from the same J'' level sum to $(2J'' + 1)$ (Kovacs 1969; Whiting et al. 1980). It follows that for each J'', the corresponding band f-value, $f(J'')$, is obtained from the sum of the corresponding P and R line f-values,

$$f = f_{J''+1,J''} + f_{J''-1,J''}. \tag{5}$$

The application of equation (5) to the line oscillator strengths of Table 1 produces the data represented by open circles in Figure 5.

In the region of the avoided crossing of $c'_4(0)$ with $b'(1)$, oscillator strength flows from the strong $c'_4(0)$–$X(0)$ transition into the very much weaker $b'(1)$–$X(0)$ band. Consequently, the sum of equation (5) must be extended to include

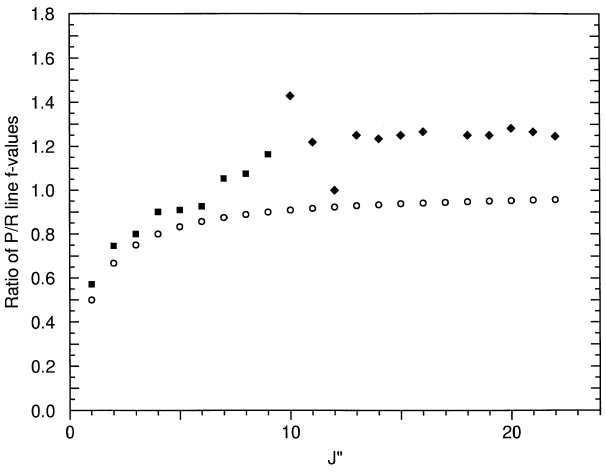

FIG. 4.—P/R ratios of the measured line f-values for $J'' \leq 9$ (*filled squares*) and $10 \leq J'' \leq 22$ (*filled diamonds*), the latter including the unresolved lines of the R head. Uncertainties in the ratios are estimated to be ~5% for $J'' < 10$, and ~10% for $J'' \geq 10$. Anomalies near $J'' = 11$ arise from the homogeneous $c'_4(0)$–$b'(1)$ interaction. Also shown are the analogous ratios of the Hönl-London factors for an unperturbed $^1\Sigma$–$^1\Sigma$ transition (*open circles*).

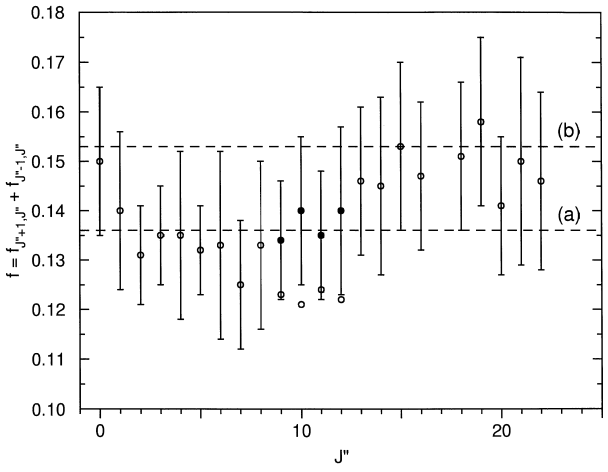

FIG. 5.—*Open circles*: The $c'_4(0) \leftarrow X(0)$ band oscillator strengths, $f(J'')$, calculated from the data in Table 1 according to eq. (5). *Filled circles*: The $f(J'')$ values inclusive of the oscillator strengths borrowed by $b'(1)$ (see Table 2) near the avoided crossing with $c'_4(0)$. The dotted horizontal lines (*a*) and (*b*) represent, respectively, the room temperature band *f*-values measured in the present work and the renormalized calculated *f*-value of Stahel et al. (1983); see Table 3.

the extra *P* and *R* lines that appear because of this local perturbation. At the low pressures used to record the 0–0 band of c'_4–X, only the six extra lines collected in Table 2 could be observed with measurable intensity. Their inclusion in the sum of equation (5) restores the $c'_4(0)$–$X(0)$ oscillator strengths derived from transitions originating in $J'' = 9,\ldots,12$ to the values shown by filled circles in Figure 5, bringing them back into line with the less strongly perturbed $f(J'')$ values measured at greater distance from the avoided crossing.

Irrespective of the large error bars that attach to the data of Figure 5, the derived band oscillator strengths are seen to display an obvious *J* dependence. At the lowest and highest *J* values, they are consistent with the renormalized (Stark et al. 1992) calculation of Stahel et al. (1983); at intermediate *J* values, they drop by about 13% to just below the room temperature *f*-value derived from the band integrated cross section (see Table 3). Stahel et al. (1983) pointed out that the high intensity of the $c'_4(0) \leftarrow X(0)$ band arises from its long-range interference with the $b'(v) \leftarrow X(0)$ transitions at shorter wavelengths, the 0–0 band of $c'_4 \leftarrow X$ gaining strength at the expense of the entire $v'' = 0$ progression of $b' \leftarrow X$ bands. Of key importance to the discussion of the interference patterns are products of vibronic quantities that can be written (Stahel et al. 1983) as

$$V_{c'b'} M_{c'X} M_{b'X} S_{c'0,b'v} S_{c'0,X0} S_{b'v,X0} , \qquad (6)$$

where the three electronic factors representing the interaction energy and transition moments precede the corresponding vibrational overlap integrals, and where the abbreviated notion c' is used for c'_4. The first and second overlap integrals involve the $c'_4(0)$ Rydberg level and are, thus, sensitive to the homogeneous mixing of the Rydberg level with the $b'(1)$ valence state perturber. The result has to be a slight reduction in the values of both integrals, in the first case on account of the orthogonality of $b'(1)$ to all $b'(v)$ levels taking part in the constructive interference with $c'_4(0)$, in the second case because of the lack of significant vibrational overlap of $b'(1)$ with $X(0)$. The reduced overlap integrals translate into a similarly reduced transfer to oscillator strength to $c'_4(0)$. In the rotating molecule, this reduction becomes dependent on *J* and will be most noticeable in the vicinity of the avoided crossing with the $b'(1)$ perturber. In a qualitative way, these expectations are born out by the data in Figure 5 where the band oscillator strengths for $c'_4(0)$–$X(0)$, $f(J'')$, are found to go through a broad minimum for rotational quantum numbers near the maximum of the $c'_4(0) \sim b'(1)$ interaction.

Considering the extent to which the interactions of the *np* Rydberg states with the *b* and *b'* valence states shape the dipole-allowed absorption spectrum of N_2, governing the rovibronic structures as well as the relative dipole strengths of the observed transitions, it must be assumed that rotation-dependent variations of the band oscillator strengths $f(J'')$ similar to those shown in Figure 5 are the rule rather than the exception. Thus, *f*-values derived from band integrated cross sections will, in general, be temperature dependent. Coupled with the inadequacies of calculating the corresponding line *f*-values from oversimplified band models that ignore the effects of homogeneous perturbations and/or heterogeneous ℓ-uncoupling interactions, this suggests that any detailed model of airglow emissions from highly excited N_2 levels should include measured, rather than calculated, line *f*-values. The data presented here for the 0–0 band of $c'_4 \leftarrow X$ are the first results of a series of experiments which aim at establishing the line *f*-values for all bands in the 86 to 99 nm region of the N_2 absorption spectrum; they will be the subject of future publications.

This work was supported in part by NASA grants NAG5-6222 to Wellesley College and NAG5-4348 to Harvard University. The measurements were carried out under the approval of the Photon Factory Advisory Committee (proposals 98G-245, 246). We thank the staff of the Photon Factory for their hospitality and assistance, and J. Ajello and D. Shemansky for helpful comments and suggestions. We also acknowledge the helpful contributions of M. Yamada and K. Yoshida during the experimental part of this work.

REFERENCES

Ajello, J. M., James, G. K., Franklin, B. O., & Shemansky, D. E. 1989, Phys. Rev. A, 40, 3524
Broadfoot, A. L., et al. 1989, Science, 246, 1459
Carroll, P. K. 1973, J. Chem. Phys., 58, 3597
Carroll, P. K., & Collins, C. P. 1969, Can. J. Phys., 47, 563
Carroll, P. K., Collins, C. P., & Yoshino, K. 1970, J. Phys. B, 3, L127
Carroll, P. K., & Yoshino, K. 1967, J. Chem. Phys., 47, 3073
———. 1972, J. Phys. B, 5, 1614
Carter, V. L. 1972, J. Chem. Phys., 56, 4195
Chan, W. F., Cooper, G., & Brion, C. E. 1991, Phys. Rev. A, 44, 186
Chan, W. F., Cooper, G., Sodhi, R. N. S., & Brion, C. E. 1993, Chem. Phys., 170, 81
Christensen, A. B. 1976, Geophys. Res. Lett., 3, 221
Dressler, K. 1969, Can. J. Phys., 47, 547
Edwards, S. A., Roncin, J.-Y., Launay, F., & Rostas, F. 1993, J. Mol. Spectrosc., 162, 257
Edwards, S. A., Tchang-Brillet, W.-U. L., Roncin, J.-Y., Launay, F., & Rostas, F. 1995, Planet. Space Sci., 43, 67
Geiger, J., & Schröder, B. 1969, J. Chem. Phys., 50, 7
Gürtler, P., Saile, V., & Koch, E. E. 1977, Chem. Phys. Lett., 48, 245

Hudson, R. D. 1971, Rev. Geophys., 9, 305
Ito, K., Maeda, K., Morioka, Y., & Namioka, T. 1989, Appl. Opt., 28, 1813
Ito, K., Namioka, T., Morioka, Y., Sasaki, T., Noda, H., Got, K., Katayama, T., & Koike, M. 1986, Appl. Opt., 25, 837
Johns, J. W. C. 1974, Specialist periodical report, Mol. Spectrosc. 2 (Chem. Soc. London), 513
Jolly, A., Lemaire, J. L., Belle-Oudry, D., Edwards, S., Malmasson, D., Vient, A., & Rostas, F. 1997, J. Phys. B, 30, 4315
Kovács, I. 1969, Rotational Structure in the Spectra of Diatomic Molecules (New York: Elsevier), 122
Lawrence, G. M., Mickey, D. L., & Dressler, K. 1968, J. Chem. Phys., 48, 1989
Lefebvre-Brion, H. 1969, Can. J. Phys., 47, 541
Levelt, P. F., & Ubachs, W. 1992, Chem. Phys., 163, 263
Meier, R. R. 1991, Space Sci. Rev., 58, 1
Morton, D. C., & Noreau, L. 1994, ApJS, 95, 301
Shemansky, D. E., Kanik, I., & Ajello, J. M. 1995, ApJ, 452, 480
Stahel, D., Leoni, M., & Dressler, K. 1983, J. Chem. Phys., 79, 2541
Stark, G., Smith, P. L., Huber, K. P., Yoshino, K., Stevens, M. H., & Ito, K. 1992, J. Chem. Phys., 97, 4809
Stark, G., Yoshino, K., Smith, P. L., Ito, K., & Parkinson, W. H. 1991, ApJ, 369, 574
Stevens, M. H., Meier, R. R., Conway, R. R., & Strobel, D. F. 1994, J. Geophys. Res., 99, 417
Stevens, M. H. 1999, J. Geophys. Res., submitted
Strobel, D. F., & Shemansky, D. E. 1982, J. Geophys. Res., 87, 1361
Ubachs, W. 1997, Chem. Phys. Lett., 268, 201
Whiting, E. E., Schadee, A., Tatum, J. B., Hougen, J. T., & Nicholls, R. W. 1980, J. Mol. Spectrosc., 80, 249
Yoshino, K., Freeman, D. E., & Tanaka, Y. 1979, J. Mol. Spectrosc., 76, 153
Yoshino, K., & Tanaka, Y. 1977, J. Mol. Spectrosc., 66, 219